

## Supplementary Information for

### **Radar-Like MoS<sub>2</sub> Nanoparticles as a High Efficient 808 nm Laser-Induced Photothermal Agent for Cancer Therapy**

Zichen Huang<sup>a</sup>, Yafei Qi<sup>b</sup>, Dexin Yu<sup>\*b</sup> and Jinhua Zhan<sup>\*a</sup>

<sup>a</sup> National Engineering Research Center for Colloidal Materials and Key Laboratory  
for Colloid and Interface Chemistry of Ministry of Education, Department of  
Chemistry, Shandong University, Jinan 250100, China.

<sup>b</sup> Qilu Hospital of Shandong University, Jinan, 250100, China

1. Synthesis of MoS<sub>2</sub> INPs.
2. Synthesis of MoS<sub>2</sub> nanoflowers.
3. Synthesis of MoS<sub>2</sub> microspheres.
4. XRD data and SEM images of other morphologies. (Fig.S1)
5. Elemental mapping plots of a single MoS<sub>2</sub> RNP. (Fig.S2)
6. Calculation of Photothermal conversion efficiency of MoS<sub>2</sub> RNPs. (Fig.S3)
7. Calculation of Photothermal conversion efficiency of other morphologies. (Fig.S4)
8. Apoptosis assay of cells without laser treatment. (Fig.S5)
9. Histological examination of tumors 7 d after the treatment. (Fig.S6)
10. Changes of tumor volume after laser treatment. (Fig.S7)

### 1. Synthesis of MoS<sub>2</sub> INPs.

0.4 mmol of sodium molybdate dihydrate (Na<sub>2</sub>MoO<sub>4</sub>·2H<sub>2</sub>O) and 1 mmol of thioacetamide (CH<sub>3</sub>CSNH<sub>2</sub>) were dissolved in 30 ml deionized water under magnetic stirring, the transparent mixture solution was then transferred into a Teflon-lined stainless steel autoclave. After sealed, the autoclave was heated to 200 °C for 72 h. The resulting products was washed by deionized water for several time, and dried overnight at 60 °C.

### 2. Synthesis of MoS<sub>2</sub> nanoflowers.

MoS<sub>2</sub> nanoflowers were synthesized by the method based on previous study. 0.53 g heptamolybdate tetrahydrate ((NH<sub>4</sub>)<sub>6</sub>Mo<sub>7</sub>O<sub>24</sub>·4H<sub>2</sub>O) and 0.46 g thiourea (CS(NH<sub>2</sub>)<sub>2</sub>) were dissolved in 35 ml of water under magnetic stirring, the mixture were then transferred into a Teflon-lined stainless steel autoclave. After sealed, the autoclave was heated to 220 °C for 24 h. The resulting products was washed by deionized water for several time, then dried at 60 °C.

### 3. Synthesis of MoS<sub>2</sub> microspheres

MoS<sub>2</sub> microspheres were synthesized by the method based on previous study. 0.484 g Na<sub>2</sub>MoO<sub>4</sub>·2H<sub>2</sub>O and 0.751 g CH<sub>3</sub>CSNH<sub>2</sub> were dissolved in 30 ml deionized water under magnetic stirring, the mixture were then transferred into a Teflon-lined stainless steel autoclave. The autoclave was heated to 240 °C for 24 h after sealed. The products was washed by deionized water and ethanol, and then dried at 40 °C under vacuum.

4. XRD data and SEM images of other morphologies.

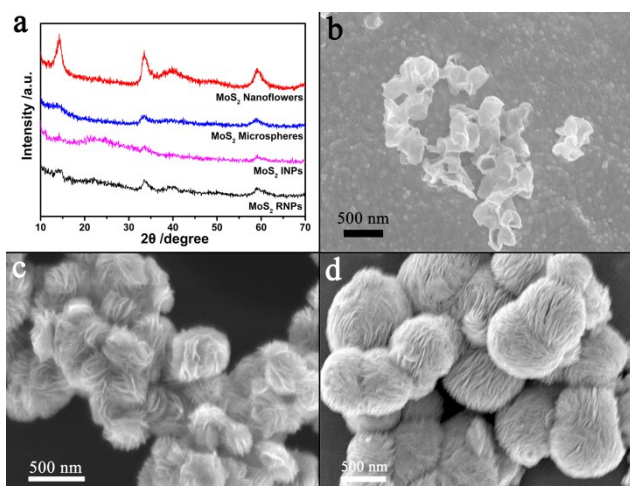


Fig. S1 (a) XRD patterns of MoS<sub>2</sub> with different morphology as noted, all the main peaks can be indexed to hexagonal phase (JCPDS 73-1508), (b-d) SEM image of the b) MoS<sub>2</sub> INPs, c) MoS<sub>2</sub> nanoflowers and d) MoS<sub>2</sub> microspheres.

5. Elemental mapping plots of a single MoS<sub>2</sub> RNP.

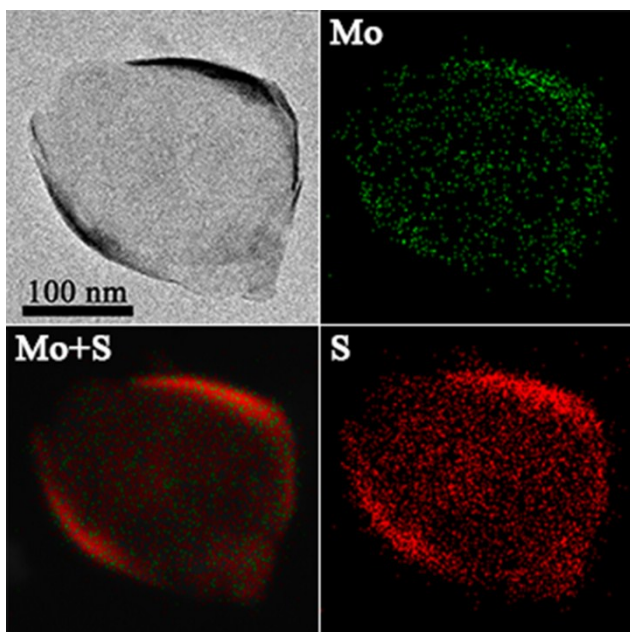


Fig S2. Elemental (Mo, S) mapping plots of a single MoS<sub>2</sub> RNP.

6. Calculation of Photothermal conversion efficiency of MoS<sub>2</sub> RNPs.

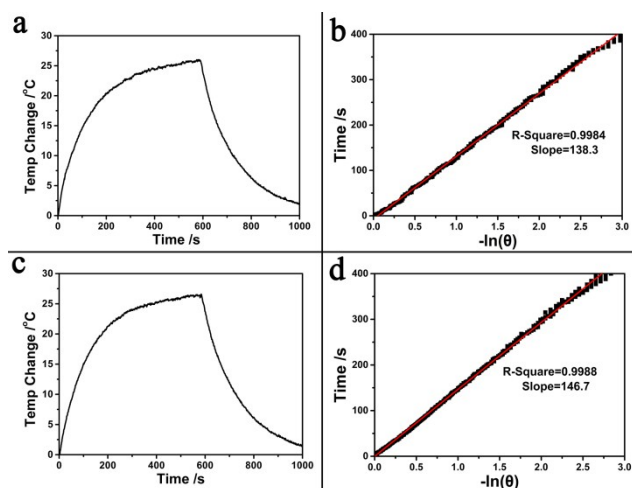


Fig S3. (a, c) Temperature change of MoS<sub>2</sub> RNPs aqueous solution (100 ppm) upon being irradiated by 808 nm laser for 600 s and shutting down the laser power, (b, d) Calculation of time constant ( $\tau_s$ ) by applying the linear time data of cooling (b from a, d from c) versus negative natural logarithm of dimensionless driving force temperature ( $\theta$ ).

7. Calculation of Photothermal conversion efficiency of other morphologies.

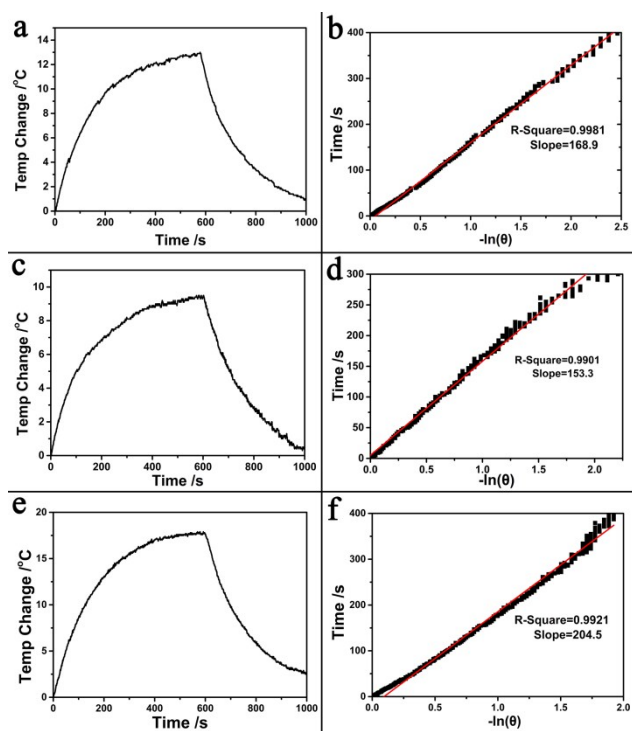


Fig S4. (a, c, e) Temperature change of MoS<sub>2</sub> nanoflowers (a), microspheres (c) and INPs (e) aqueous solution (100 ppm) upon being irradiated by 808 nm laser for 600 s and shutting down the laser power, (b, d, f) Calculation of time constant ( $\tau_s$ ) by applying the linear time data of cooling (b from a, d from c, f from e) versus negative natural logarithm of dimensionless driving force temperature ( $\theta$ ).

8. Apoptosis assay of cells without laser treatment.

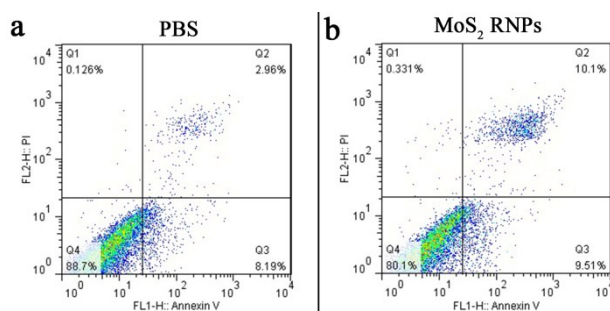


Fig S5. Flow cytometric analysis for apoptosis of 4T1 cells treated with PBS (a) and MoS<sub>2</sub> RNPs (b) without laser treatment.

9. Histological examination of tumors 7 d after the treatment.

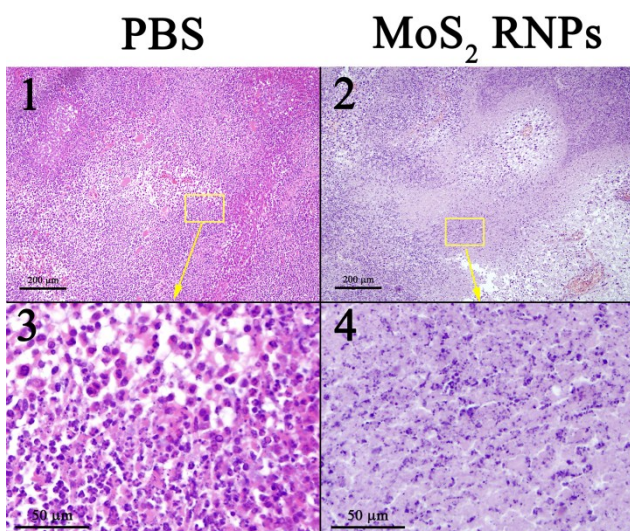


Fig S6. Histological images of tumor tissues obtained from control group (1 and 3) and experimental group (2 and 4) 7 d after the treatment. A considerable region of karyolysis can be observed in 4.

10. Changes of tumor volume after laser treatment. (Fig.S7)

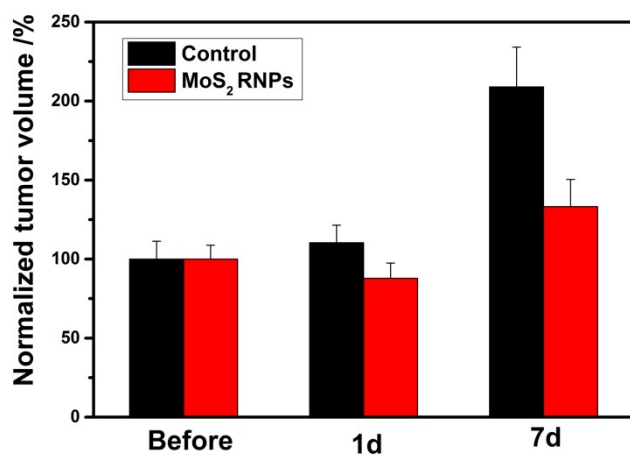


Fig S7. Changes of tumor volume after laser treatment, experimental group treated with MoS<sub>2</sub> RNPs exhibit a volume decrease 1d after irradiation; furthermore, the lesser normalized volume 7d after irradiation indicated that the tumor growth rate of experimental group was reduced due to the treatment.